

# Durability and physical characterization of anti-fogging solution for 3D-printed clear masks and face shields

Succhay Gadhar<sup>Equal first author, 1</sup>, Shaina Chechang<sup>Equal first author, 1</sup>, Philip Sales<sup>1</sup>, Praveen Arany<sup>Corresp. 1</sup>

<sup>1</sup> Oral Biology, Biomedical Engineering, and Surgery, University at Buffalo, Buffalo, NY, USA

Corresponding Author: Praveen Arany  
Email address: praveenarany@gmail.com

**Background.** The COVID-19 pandemic brought forth the crucial roles of personal protective equipment (PPE) such as face masks and shields. Additive manufacturing with 3D printing enabled customization and generation of transparent PPEs. However, these devices were prone to condensation from normal breathing. This study was motivated to seek a safe, non-toxic, and durable anti-fogging solution. **Methods.** We used additive 3D printing to generate the testing apparatus for contact angle, sliding angle, and surface contact testing. We examined several formulations of carnauba wax to beeswax in different solvents and spray-coated them on PETG transparent sheets for testing contact and sliding angle, and transmittance. Further, the integrity of this surface following several disinfection methods such as soap, Isopropyl Alcohol, or water alone with gauze, paper towels, and microfiber, along with disinfectant wipes, was assessed. **Results.** The results indicate a 1 : 2 ratio of carnauba to beeswax in Acetone optimally generated a highly hydrophobic surface (contact angle  $150.3 \pm 2.1^\circ$  and sliding angle  $13.7 \pm 2.1^\circ$ ) with maximal transmittance. The use of soap for disinfection resulted in the complete removal of the anti-fogging coating, while Isopropyl Alcohol and gauze optimally maintained the integrity of the coated surface. Finally, the contact surface testing apparatus generated a light touch ( $5000 \text{ N/m}^2$ ) that demonstrated good integrity of the antifogging surface. **Conclusions:** This study demonstrates that a simple natural wax hydrophobic formulation can serve as a safe, non-toxic, and sustainable anti-fogging coating for clear PPEs compared to several commercial solutions.

1     **Durability and Physical Characterization of Anti-Fogging**  
2     **Solution for 3D-Printed Clear Masks and Face Shields**

3             Succhay Gadhar<sup>1,\*</sup>, Shaina Chechang<sup>1,\*</sup>, Philip Sales<sup>1</sup>, Praveen R. Arany<sup>1,\$</sup>

4             <sup>1</sup> Oral Biology, Biomedical Engineering and Surgery, University at Buffalo, NY, USA

5     \* *Equal contributions*

6

7     <sup>\$</sup>**Address correspondence to:**

8     Praveen R. Arany B.D.S., M.D.S., M.M.Sc., Ph.D.

9     3435 Main Street, BRB 553,

10    Buffalo, NY 14214.

11    E-mail: [prarany@buffalo.edu](mailto:prarany@buffalo.edu)

12    Phone: 716-829-3479

13

14

15    **Keywords:** Face shields, Masks, Anti-fogging

16

17

18

19 **ABSTRACT**

20 **Background.** The COVID-19 pandemic brought forth the crucial roles of personal protective  
21 equipment (PPE) such as face masks and shields. Additive manufacturing with 3D printing enabled  
22 customization and generation of transparent PPEs. However, these devices were prone to  
23 condensation from normal breathing. This study was motivated to seek a safe, non-toxic, and  
24 durable anti-fogging solution.

25 **Methods.** We used additive 3D printing to generate the testing apparatus for contact angle, sliding  
26 angle, and surface contact testing. We examined several formulations of carnauba wax to beeswax  
27 in different solvents and spray-coated them on PETG transparent sheets for testing contact and  
28 sliding angle, and transmittance. Further, the integrity of this surface following several disinfection  
29 methods such as soap, Isopropyl Alcohol, or water alone with gauze, paper towels, and microfiber,  
30 along with disinfectant wipes, was assessed.

31 **Results.** The results indicate a 1 : 2 ratio of carnauba to beeswax in Acetone optimally generated  
32 a highly hydrophobic surface (contact angle  $150.3 \pm 2.1^\circ$  and sliding angle  $13.7 \pm 2.1^\circ$ ) with  
33 maximal transmittance. The use of soap for disinfection resulted in the complete removal of the  
34 anti-fogging coating, while Isopropyl Alcohol and gauze optimally maintained the integrity of the  
35 coated surface. Finally, the contact surface testing apparatus generated a light touch ( $5000 \text{ N/m}^2$ )  
36 that demonstrated good integrity of the antifogging surface.

37 **Conclusions:** This study demonstrates that a simple natural wax hydrophobic formulation can  
38 serve as a safe, non-toxic, and sustainable anti-fogging coating for clear PPEs compared to several  
39 commercial solutions.

40

41

42

43

44

45

## 46 INTRODUCTION

47 The COVID-19 pandemic has had a significant toll on the public health, biomedical, and  
48 financial aspects that have significantly changed society.(1,2) Among various healthcare services,  
49 the presence of SARS-CoV in the nasal and upper respiratory tract presented significant challenges  
50 for dentists and anesthetists. Clinical dentistry presented a significant challenge due to the  
51 proximity and inherent aerosol-generating procedures. (3-5) The use of personal protection  
52 equipment (PPE) such as face masks and face shields was integral in reducing the spread of  
53 infections among the general population. (6) While dentistry routinely utilizes face masks, double  
54 masking, and the highly protective N95, the shielding nature and the lack of face-to face exposure  
55 further compounded the pandemic fear and anxiety in patients naturally apprehensive about their  
56 dental visits. (7-9) Another major limitation of these masks is that they hinder effective  
57 communication due to the lack of non-verbal cues such as facial expressions and lips movements.  
58 (10-12) This is particularly challenging in patients with differently-abled hearing due to increased  
59 signal-to-noise from the ambient noise in dental operatories. (13-16) The use of transparent masks  
60 and face shields has been demonstrated to improve these limitations. (17)

61 Another major challenge during the early phase of the pandemic was the significant  
62 disruption of the PPE supply chain requiring local innovations where additive manufacturing using  
63 3D printing came to the forefront. (18-21) The ability to generate required quantities based on need  
64 and additional customization for individual applications were significant advantages of this  
65 approach. (22) Building on this, in collaboration with e-NABLE, a 3D printing community,  
66 students at the University at Buffalo School of Dental Medicine generated transparent PPEs using  
67 3D printing and vacuum casting. Among them, several custom designs were specifically generated  
68 to accommodate commercially available dental loupes that are made available freely online.(23)  
69 These clear masks and face shields were well accepted and generated much enthusiasm among  
70 clinical users. Besides dentistry, another group of clinicians that notably adopted these clear PPEs  
71 were the local speech and hearing-impaired clinics. However, an immediate limitation of this  
72 approach reported by users was the fogging due to the moisture from regular breathing. This  
73 essentially negated the advantage of the transparent nature of these masks and face shields and  
74 presented additional hindrance of needing repetitive wipe-downs.

75           The commercially available anti-fogging solutions used for eyeglasses and car exteriors  
76 contain polydimethylsiloxane and silica nanoparticles. The long-term use of these solutions was  
77 considered unsuitable due to their potential for skin irritation, and potential inhalation or ingestion.  
78 Hence, we sought to identify a non-toxic, antifogging coating for the transparent masks and face  
79 shields for long-term use. To design such a solution, specific design criteria needed to be met. The  
80 surface of a water droplet is attracted to the bulk of the droplet due to cohesion which results in  
81 their beading. The shape that a drop takes on a given surface depends on the surface tension of the  
82 fluid and the physical characteristics of the surface. A surface-fluid interface is the contact angle  
83 that measures the wettability of a surface. Contact angles can vary from hydrophilic (less than or  
84 equal to  $30^\circ$ ) to hydrophobic (greater than or equal to  $120^\circ$ ), where the higher the contact angle,  
85 the lower its wettability. (24) Another measure of the extent of moisture retention on a surface is  
86 the sliding angle which is measured by tilting the surface with the solution bead to determine the  
87 angle at which it rolls off. The more hydrophobic the surface, the higher the angle of loss of fluid  
88 droplets. (25) Another key design aspect of the anti-fogging solution would be its resistance to wear  
89 due to repeated skin surface contact during mask use. The ideal solution would offer a thin, durable  
90 coating for daily use that would not need repetitive applications while maintaining maximal  
91 transparency.

92           Natural products offer attractive non-toxic coatings. Prior studies have examined the  
93 combination of cinnamon and nutmeg that produces high hydrophobicity. (26) Although both are  
94 natural products, this paper utilized a organosilane-based alkyl and perfluorinated synthetic  
95 chemical coatings that raised some toxicity concerns due to high cuprous oxide content. We drew  
96 inspiration from the naturally occurring, extremely hydrophobic lotus leaves. These leaves expel  
97 water easily due to their micro-structural features, termed papillae, that exude epicuticular waxes,  
98 cutin. (27,28) Alternatively, Carnauba and beeswax have also high hydrophobicity that are  
99 routinely used in the food service industry. (29) With their high hydrophobicity, these solutions on  
100 food containers prevent waste by ensuring minimal food retention. However, there was a lack of  
101 clarity in the concentrations used in these prior formulations and the resulting hydrophobicity. The  
102 present study examined the different formulations of these two waxes together and evaluated the  
103 contact angle, sliding angle, and transmittance. The optimized formulation was subjected to  
104 durability testing with manual disinfectant procedures and long-term contact-wear testing.

## 105 MATERIALS AND METHODS

### 106 Formulation of anti-fogging solutions

107 Hydrophobic wax coatings were generated in acetone or methanol as solvents using  
108 ultrasonication. Different ratios of carnauba wax to beeswax (both Sigma Aldrich, St. Louis, MO)  
109 were employed namely 0.4375 g: 0.4375 g (1:1), 0.35 g: 0.525 g (1:1.5), 0.33 g: 0.66 g (1:2), 0.417  
110 g: 0.834 g (1:2HC) were melted in a 50 ml plastic tube (Corning, Thermofisher Waltham, MA) in  
111 a water bath. After the waxes had melted, 25 milliliters of either acetone or methanol (both Sigma  
112 Aldrich, St. Louis, MO) were added, and the solution was emulsified immediately using a probe  
113 ultrasonication (Q2000, QSonica, Newtown CT) at 90% amplitude for 3 minutes and transferred  
114 into a 2 oz glass spray bottle.

### 115 Contact and Sliding Angle testing

116 Solutions were sprayed onto a 2 x 2-inch sheet of PETG at roughly a distance of 5 inches, spraying  
117 10 times. After drying, the sheets of PETG were tested for contact angle, sliding angle, and  
118 transmission. A custom contact and sliding angle device were generated based on commercially  
119 available models using online CAD software (Onshape, PTC, Rockwell Automation, Boston MA).  
120 The devices were printed using Polylactic acid (PLA) filament (Overture, Overture 3D  
121 Technologies, Texas) on a i3 Prusa 3D printer (Prusa Research, Prague Czech Republic) (**Figs. 1**  
122 **A - C**). The device included a slot for to hold a mobile phone to take digital pictures of the droplet.  
123 After fixing the plastic surface to the platform, droplets of water were generated with a 3 ml syringe  
124 and 14-gauge needle (to mimic humidity post-condensation on clear PPEs) and digital image were  
125 captured for analysis (**Fig. 1 D**). The digital images were analyzed using the NIH ImageJ (ver.  
126 1.53n) software. The sliding angle set up included a protractor to assess the angle at which the  
127 droplet slides off. The platform was tilted slowly until the water droplet slid off, and the angle was  
128 documented (**Fig. 1 E**). All studies were performed in performed in triplicate and repeated at least  
129 twice.

### 130 Transmittance analysis

131 The laser apparatus consisted of a 650 nm diode laser (Weber Medical, Beverungen, Germany) at  
132 10 mW/cm<sup>2</sup>, and a sensor with power meter (both Thor Labs, Newton NJ) (**Fig. 1F**). The sheets  
133 of PETG were placed on top of the power sensor, and transmission was assessed.

**134 Optical clarity analysis**

135 A sticker was placed on a bench and the sheets of PETG were placed over it. Digital pictures were  
136 taken with a mobile phone camera. The coated sheets of PETG were compared with the uncoated  
137 control and the visual clarity of the coatings was assessed.

**138 Routine manual disinfection testing**

139 The PETG coated surfaces were subjected to different solutions such as soap solution (10% v/v,  
140 Dawn, Procter & Gamble, Cincinnati OH), Isopropyl alcohol (70%, Sigma Aldrich, St. Louis MO),  
141 and water alone using paper towels (Uline, Milton ON), gauge (Henry Schein, New York, NY) or  
142 microfibers (Magic Fiber, Miami FL). These disinfectants were applied ten times in a uniform,  
143 lateral motion with manual pressure by a single operator. Disinfection wipes (Metrex, Orange CA)  
144 were used in another group.

**145 Coating Durability following contact wear testing**

146 To simulate accelerated contact wear testing, a custom apparatus was designed to mimic skin  
147 contact. Using the CAD software (Onshape, PTC, Rockwell Automation, Boston MA), a rotating  
148 platform with spring-loaded bases was designed to apply suitable skin contact forces. (30-32) The  
149 device was 3D printed with PLA filament (Overture, Overture 3D Technologies, Texas) on a i3  
150 Prusa 3D printer (Prusa Research, Prague Czech Republic). The wheel was connected to a DC  
151 Motor (Greartisan, Shenzhen Hotec, China) via a speed controller and a 9V battery which allowed  
152 the motor to function up to 1000 RPMs. After the coated samples were mounted on the platforms,  
153 the apparatus was positioned to allow the platforms to extend and retract using centrifugal force  
154 while spinning, hitting a skin-equivalent surface (rough side of oil-treated leather) to simulate  
155 contact. To simulate multiple skin contacts, the device was operated for 5 minutes, allowing each  
156 platform to contact the wall about 5000 times for each sample. The contact force applied by the  
157 rotational, spring-loaded platform was measured with a digital force probe (Baoshishan, China).  
158 Following the contact wear testing, samples were assessed for changes in contact angle, sliding  
159 angle, transmittance and examined with topological analysis.

160

161

## 162 **Topological analysis**

163 Scanning electron microscopy (SEM) analysis was performed to determine the topology and the  
164 depth of the coating on the plastic sheet samples prior to and following wear testing. Samples were  
165 sputter-coated (Cressington 108, Ted Pella Inc, Redding CA) with carbon for 120 seconds and  
166 examined using SEM (Hitachi, S-4700, Japan) with a voltage of 2.0 kV at about  $14.5 \pm 0.4$  mm  
167 using secondary electron mode.

## 168 **Statistical Analysis**

169 Data was organized in Excel (Microsoft, Seattle WA) and presented as Means with standard  
170 deviations. Data was subjected to a Student's T test or two-way analysis of variance (ANOVA)  
171 among different treatments with Bonferroni's correction for multiple comparisons where  
172 appropriate. A  $p < 0.05$  was considered statistically significant.

## 173 **RESULTS**

### 174 **Formulation and Characterization of Anti-Fogging solutions**

175 We first examined different ratios of carnauba and beeswax in two solvents namely  
176 Acetone and Ethanol to generate a homogenous solution (**Fig. 2A**). The contact angles of the  
177 acetone-based solutions were higher than their methanol counterparts (**Figs. 2B** and **2C**). The  
178 coating with the highest contact angle was the 1: 2 ratio in acetone solution with a mean contact  
179 angle of  $150.3 \pm 2.1$  °. This categorizes this surface coating as highly hydrophobic compared to  
180 the other coatings and was significantly ( $p < 0.05$ ) more hydrophobic than the uncoated plastic  
181 surface. We also examined the higher concentrations (HC) at 1 : 2 ratio to inquire if the density  
182 and hence, eventual coating concentration would affect these properties, but did not observe any  
183 further significantly improved characteristics. As expected the sliding angle for this coating was  
184 the lowest at  $13.7 \pm 2.1$ ° which was significantly ( $p < 0.05$ ) lower than the uncoated plastic surface  
185 (**Figs. 2D** and **2E**). The transmittance of these formulation appears to vary with the concentration  
186 of the beeswax component as lower amounts resulted in higher transmittance (**Figs. 2F** and **2G**).  
187 The optical clarity was also assessed through the observation of the sticker through the coated  
188 slides. The optical clarity decreased as the concentrations of the solutes increased as was expected.  
189 The methanol-based formulations had a higher degree of transmittance than the acetone

190 counterparts. Based on these results, we decided to pursue the 1:2 carnauba to bee wax in acetone  
191 formulation for subsequent studies.

### 192 **Effect of routine disinfection procedures on durability of antifogging solution**

193 The use of disinfectants is a necessary part of routine plastic mask and face shield use due  
194 to the prominent aerosol generating dental procedures. (33-35) Next, we examined routine  
195 disinfectant procedures employed in the dental office namely, soapy water, 70% Isopropyl Alcohol  
196 with paper towels, gauze, or microfiber, and disinfectant wipes. We noted a significant ( $p < 0.05$ )  
197 reduction in the contact angle after all disinfection methods (**Fig. 3A**). Among all these methods,  
198 Isopropyl Alcohol with gauze reduced the contact angle the least ( $144.3 \pm 1.6^\circ$ ) while soap made  
199 the surface most hydrophilic (wettable). Concurrently, the sliding angle analysis showed a similar  
200 trend, increasing overall with all, but the soap group, disinfection methods (**Fig. 3B**). The Isopropyl  
201 alcohol group showed the least change and no statistically significant difference was noted with  
202 the paper towel method. Interestingly, the transmittance appeared to vary after individual  
203 disinfectant methods with some showing increases while other showing significant decreases (**Fig.**  
204 **3C**). The method of disinfection that showed most increase in light transmission was wipes alone  
205 while the most reduction was observed with Isopropyl Alcohol and paper towel method. These  
206 results suggest that using Isopropyl Alcohol with gauze is optimal for disinfection as it minimally  
207 affects antifogging coating properties after repeated use.

### 208 **Antifogging coating stability after contact wear testing**

209 Finally, we investigated the durability of the anti-fogging solutions as they would be  
210 subjected to rigorous daily wear and tear during PPE use. We first created a simple rig to simulate  
211 skin contact based on a 3D printed apparatus (**Fig. 4A and B**). The rig was designed as a rotating  
212 platform that would result in a repetitive contact of the coated device with a stationary leather  
213 surface. The pressure exerted by facemask on the nose bridge and chin contact has been assessed  
214 to be 45 to 91 mm of Hg ( $6000\text{-}12,000\text{ N/m}^2$ ) (**Fig. 4C**). (30-32) The constant skin contact force  
215 in our device was assessed to be  $5000\text{ N/m}^2$  that could be approximated to a repeated light skin  
216 contact.

217 Following the simulated wear, the contact and sliding angle as well as transmittance was  
218 assessed. We observed a significant reduction in contact angle ( $133.3 \pm 1.5^\circ$ ) and concomitant

219 increase in the sliding angle ( $23.7 \pm 1.5^\circ$ ) compared to the uncoated control surfaces. While  
220 transmittance was not significantly different before and after wear simulation, there was a trend  
221 towards reduced transmission. Topological analysis noted the wear simulation resulted in  
222 significant accretions and scratches that likely contribute to the reduced light transmission  
223 observed. These results indicate the coating will likely need to be replaced over repeated PPE use  
224 as often as every other week.

225

## 226 **DISCUSSION**

227 The COVID pandemic presented new challenges to healthcare with an urgent need for  
228 innovations in disinfection approaches. The use of PPE was central in the attempts to mitigate the  
229 spread of infection and a major part of the solution to mitigate the health crisis. The use of these  
230 barriers continues to have an impact on both the psychological, and medical well-being of both the  
231 patients and the healthcare professionals themselves.(36) The initial response to the pandemic  
232 brought manufacturing and supply chain disruptions resulting in additive 3D printing enthusiasts  
233 to offer custom, local solutions. Our team at the University at Buffalo focused on the transparent  
234 PPE designs and dental loop attachments (**Fig. 5**). The condensation from breathing obscured the  
235 functions of the clear PPEs that presented a major impasse to their use. This work was specifically  
236 motivated to address this deterrent to routine clear PPE use.

237 We tested polyethylene terephthalate glycol (PETG). PETG is a commonly-used  
238 thermoplastic with impact resistance, durability, ductility, chemical resistance properties well-  
239 suited to this application. To generate an anti-fogging solution for our clear face shields and masks,  
240 a major design challenge was the close proximity to nose and mouth.(37,38) We chose to pursue  
241 natural waxes as the main ingredient as they provided a natural, non-toxic solution that has a well-  
242 established track record of biological safety. (39) The other major component constituent was a  
243 polar solvent to enhance miscibility and dispersion of these waxes. We chose to examine Acetone  
244 and Ethanol in our formulation. The acetone formulation was superior in generating the most  
245 hydrophobic product after spray coating. Our initial efforts at dissolving the waxes in Acetone  
246 (boiling point of  $132.8^\circ\text{F}$ ) by heating alone resulted in evaporation and non-uniform dissolution.  
247 Hence, we chose to disperse the waxes via ultrasonication. Among the various formulations, the  
248 most hydrophobic surface was generated by the 1 : 2 ratio (contact angle  $150.3 \pm 2.1^\circ$ ) though the

249 other formulations were also strongly hydrophobic (contact angles 121 to 135°). We also examined  
250 Methanol (boiling point of 148.5 °F) in the same volume that, in contrast, generated hydrophilic  
251 surface coatings with all formulations (contact angles 34 to 82 °), but most prominently with the 1  
252 : 2 at the higher concentration (contact angle  $80.7 \pm 2.1$  °). Increasing the concentration in the  
253 Methanol formulation (1 : 2 HC) appeared to impact the physical characteristics more than the  
254 Acetone (1 : 2 HC) formulation that could be attributed to differential dissolution of the waxes and  
255 subsequent homogeneity of the coating film. Among the two solvents examined, Methanol did not  
256 enable a suitable anti-fogging formulation and hence, the 1: 2 formulation in Acetone was chosen  
257 as an optimal anti-fogging solution. This may have been due to the fact that methanol has a higher  
258 polarity than acetone that facilitates improved dispersibility of the non-polar wax compounds.

259         The use of surface disinfectants is an integral part of maintaining and reusing PPEs. This  
260 is a sustainable and cost-effective practice that is routinely employed. A key design requirement  
261 of the anti-fogging solution is durability with these disinfectant approaches. We observed that the  
262 soap solution group consistently demonstrated complete removal of the anti-fogging solution.  
263 While this desirable as a disinfectant approach to remove all potentially hazardous aerosols on  
264 these PPEs, its amphiphilic nature allowing it to form micelles with the wax components of the  
265 anti-fogging solution would deem it unsuitable. The removal of the anti-fogging solution with  
266 these approaches could be attributed to the surfactant nature that interferes with the surface tension  
267 of the water droplets. Another possibility is that the lipid-to-lipid interaction of the soap and the  
268 waxes may inactivate the hydrophobic nature of the coating. The superior solubilizing ability of  
269 isopropyl alcohol that may further smoothen the coating, reduce surface tension further or alter  
270 drying times are areas of future investigations.

271         To investigate the durability of the anti-fogging coating, we generated a custom rig for  
272 accelerated surface contact testing. The major design principle for this device was to generate a  
273 PPE skin contact force. The reported PPE skin contact force to create a tight seal on the nose and  
274 chin has been reported as 45 to 91 mm of Hg (6000-12,000 N/m<sup>2</sup>). (30-32) The force generated by  
275 our rig was lower at 5000 N/m<sup>2</sup> and was intended to approximate light skin contact force in non-  
276 fastened areas. This reflects routine surface contact during routine use of the PPEs. The  
277 hydrophobicity of the anti-fogging surfaces was relatively well maintained (contact angle  $133.3 \pm$   
278  $1.5$ ° and sliding angle  $23.7 \pm 1.5$ °). However, the durability testing noted a reduction in the

279 transmittance of the masks that could be attributed the wear from the contact forces. As evident in  
280 the ultrastructural analysis, the PETG surface appears to have several accretions and disruption of  
281 the uniform coated surfaces. Given these PPEs are disposable and have a limited time of use, this  
282 may not significantly impact the PPE performance. In fact, this lack of clarity from routine use  
283 may be a good marker for replacement with a simple optical interferometry device.

284         This study has a few limitations. First, the biological performance of this anti-fogging  
285 solution could be examined using *in vitro* (reconstructed human epidermis), and *in vivo* skin  
286 contact testing in animals and human studies. (40-46) While this could be considered routine  
287 diligence, it is prudent to emphasize both the waxes and PETG are generally regarded as safe (FDA  
288 GRAS) and are used in current product (e.g; lip balm) formulations routinely. The solvents are  
289 readily eliminated by mild heating (40°C overnight). Second, applying a hydrophobic solution on  
290 the PETG clear surface may, counter to its primary objective, worsen the visibility due to the  
291 moisture coalescing into larger water beads. It is conceivable that the increasing size of these water  
292 beads may eventually reach a critical mass and cause them to slide off. This phenomenon is  
293 observed on hydrophobic surfaces like lotus leaves and commercial car wax coatings. Hence, a  
294 replaceable absorbent liner and a mild, mechanical vibration module to promote water droplet  
295 beading and run-off could be attractive future design iteration in these clear PPEs. Third, a major  
296 shortcoming of using such an anti-fogging spray is its temporary nature and the need for  
297 continuous replacement throughout the lifetime of the clear PPE. Thus, a potential future  
298 possibility is to pursue nanopatterning, simulating the lotus leaf papillae for a more biocompatible,  
299 permanent anti-fogging solution.

## 300 **Conclusions**

301         In summary, this work demonstrates the utility of an anti-fogging formulation with two  
302 natural waxes that has good durability and optimal non-fouling properties. This solution represents  
303 a cost-effective, durable, non-toxic approach to prevent or reduce fogging of clear PPEs such as  
304 plastic masks and face shields from condensations of humidity arising from breathing and  
305 speaking.

## 306 **Conflicts of Interests**

307 The authors declare they have no relevant conflicts of interest with this work.

## 308 Acknowledgements

309 We thank the members of the Buffalo3DPPE for their time and effort during the pandemic namely,  
310 Kierra Bleyle, Preethi Singh, Jason Ciano, Savannah Tomaka, Jacob Graca, Hunter Rosa, Yianni  
311 Savidis, Danielle Detwiler, Omer Hillel, and Georgia Kyriacou. We also thank the Buffalo Enable  
312 (BE Mask) team for their valuable collaboration and technical assistance with 3D printing namely  
313 Aaron Gorsline, Albert Titus, James Whitlock, Peter Elkin, Jeremy Simon, Jon Schull, Ben Rubin,  
314 Kelly Cheattle, Pete Suffoletto, and Skip Meetze. We would like to thank Mr. Peter Bush, South  
315 Campus Instrument core for assisting with the SEM analysis and Weber Medical laser for  
316 providing their laser device. This work was supported by the BlueSky, University at Buffalo, and  
317 Dean's fund, School of Dental Medicine.

318

## 319 References

- 320 1. Pak A, Adegboye OA, Adekunle AI, Rahman KM, McBryde ES, Eisen DP. Economic Consequences  
321 of the COVID-19 Outbreak: the Need for Epidemic Preparedness. *Front Public Health* 2020; 8:241.
- 322 2. Pirasteh-Anosheh H, Parnian A, Spasiano D, Race M, Ashraf M. Haloculture: A system to mitigate  
323 the negative impacts of pandemics on the environment, society and economy, emphasizing  
324 COVID-19. *Environ Res* 2021; 198:111228.
- 325 3. Goriuc A, Sandu D, Tatarciuc M, Luchian I. The Impact of the COVID-19 Pandemic on Dentistry and  
326 Dental Education: A Narrative Review. *Int J Environ Res Public Health* 2022; 19(5).
- 327 4. Kurian N, Gandhi S, Thomas AM. COVID-19 and multidisciplinary dentistry. *Br Dent J* 2021;  
328 231(9):534.
- 329 5. Lieberthal B, McCauley LK, Feldman CA, Fine DH. COVID-19 and Dentistry: Biological  
330 Considerations, Testing Strategies, Issues, and Regulations. *Compend Contin Educ Dent* 2021;  
331 42(6):290-296; quiz 297.
- 332 6. Artenstein AW. In Pursuit of PPE. *N Engl J Med* 2020; 382(18):e46.
- 333 7. Marcus K, Balasubramanian M, Short SD, Sohn W. Dental hesitancy: a qualitative study of  
334 culturally and linguistically diverse mothers. *BMC Public Health* 2022; 22(1):2199.
- 335 8. Muneer MU, Ismail F, Munir N, Shakoor A, Das G, Ahmed AR, Ahmed MA. Dental Anxiety and  
336 Influencing Factors in Adults. *Healthcare (Basel)* 2022; 10(12).
- 337 9. Nikolic M, Mitic A, Petrovic J, Dimitrijevic D, Popovic J, Barac R, Todorovic A. COVID-19: Another  
338 Cause of Dental Anxiety? *Med Sci Monit* 2022; 28:e936535.
- 339 10. Blais C, Fiset D, Roy C, Saumure Regimbald C, Gosselin F. Eye fixation patterns for categorizing  
340 static and dynamic facial expressions. *Emotion* 2017; 17(7):1107-1119.
- 341 11. Chodosh J, Weinstein BE, Blustein J. Face masks can be devastating for people with hearing loss.  
342 *BMJ* 2020; 370:m2683.
- 343 12. Chu JN, Collins JE, Chen TT, Chai PR, Dadabhoy F, Byrne JD, Wentworth A, DeAndrea-Lazarus IA,  
344 Moreland CJ, Wilson JAB, Booth A, Ghenand O, Hur C, Traverso G. Patient and Health Care Worker  
345 Perceptions of Communication and Ability to Identify Emotion When Wearing Standard and  
346 Transparent Masks. *JAMA Netw Open* 2021; 4(11):e2135386.

- 347 13. Fleming JT, Maddox RK, Shinn-Cunningham BG. Spatial alignment between faces and voices  
348 improves selective attention to audio-visual speech. *J Acoust Soc Am* 2021; 150(4):3085.
- 349 14. MacLeod A, Summerfield Q. Quantifying the contribution of vision to speech perception in noise.  
350 *Br J Audiol* 1987; 21(2):131-141.
- 351 15. Schwartz JL, Berthommier F, Savariaux C. Seeing to hear better: evidence for early audio-visual  
352 interactions in speech identification. *Cognition* 2004; 93(2):B69-78.
- 353 16. Sonnichsen R, Llorach To G, Hochmuth S, Hohmann V, Radeloff A. How Face Masks Interfere With  
354 Speech Understanding of Normal-Hearing Individuals: Vision Makes the Difference. *Otol Neurotol*  
355 2022; 43(3):282-288.
- 356 17. Atcherson SR, Mendel LL, Baltimore WJ, Patro C, Lee S, Pousson M, Spann MJ. The Effect of  
357 Conventional and Transparent Surgical Masks on Speech Understanding in Individuals with and  
358 without Hearing Loss. *J Am Acad Audiol* 2017; 28(1):58-67.
- 359 18. Belhouideg S. Impact of 3D printed medical equipment on the management of the Covid19  
360 pandemic. *Int J Health Plann Manage* 2020; 35(5):1014-1022.
- 361 19. O'Connor S, Mathew S, Dave F, Tormey D, Parsons U, Gavin M, Nama PM, Moran R, Rooney M,  
362 McMorro R, Bartlett J, Pillai SC. COVID-19: Rapid prototyping and production of face shields via  
363 flat, laser-cut, and 3D-printed models. *Results Eng* 2022; 14:100452.
- 364 20. Rupesh Kumar J, Mayandi K, Joe Patrick Gnanaraj S, Chandrasekar K, Sethu Ramalingam P. A  
365 critical review of an additive manufacturing role in Covid-19 epidemic. *Mater Today Proc* 2022;  
366 68:1521-1527.
- 367 21. Vallatos A, Maguire JM, Pilavakis N, Cerniauskas G, Sturtivant A, Speakman AJ, Gourlay S, Inglis S,  
368 McCall G, Davie A, Boyd M, Tavares AAS, Doherty C, Roberts S, Aitken P, Mason M, Cummings S,  
369 Mullen A, Paterson G, Proudfoot M, Brady S, Kesterton S, Queen F, Fletcher S, Sherlock A, Dunn  
370 KE. Adaptive Manufacturing for Healthcare During the COVID-19 Emergency and Beyond. *Front*  
371 *Med Technol* 2021; 3:702526.
- 372 22. Kalkal A, Allawadhi P, Kumar P, Sehgal A, Verma A, Pawar K, Pradhan R, Paital B, Packirisamy G.  
373 Sensing and 3D printing technologies in personalized healthcare for the management of health  
374 crises including the COVID-19 outbreak. *Sens Int* 2022; 3:100180.
- 375 23. Arany PSaP. Dental Faceshields. 2020.
- 376 24. Laurén S. Contact angle measurements on superhydrophobic surfaces in practice. *Surface Science*  
377 *Blog: Biolin Scientific*; 2019.
- 378 25. Lv C, Yang C, Hao P, He F, Zheng Q. Sliding of water droplets on microstructured hydrophobic  
379 surfaces. *Langmuir* 2010; 26(11):8704-8708.
- 380 26. Razavi SMR OJ, Sett S, et al. Superhydrophobic Surfaces Made from Naturally Derived  
381 Hydrophobic Materials. *ACS Sustainable Chem Eng* 2016.
- 382 27. Bormashenko E. Wetting of real solid surfaces: new glance on well-known problems. *Colloid and*  
383 *Polymer Science* 2013.
- 384 28. Li P. Submillimeter Papillae: Shape Control of Lotus Leaf Induced by Surface Submillimeter  
385 Texture. *Advanced Materials Interfaces* 2020.
- 386 29. Wang P QX, Shen J. Superhydrophobic Coatings with Edible Biowaxes for Reducing or Eliminating  
387 Liquid Residues of Foods and Drinks in Containers. *Bioresources* 2018.
- 388 30. Brill AK, Pickersgill R, Moghal M, Morrell MJ, Simonds AK. Mask pressure effects on the nasal  
389 bridge during short-term noninvasive ventilation. *ERJ Open Res* 2018; 4(2).
- 390 31. Dellweg D, Hochrainer D, Klauke M, Kerl J, Eiger G, Kohler D. Determinants of skin contact pressure  
391 formation during non-invasive ventilation. *J Biomech* 2010; 43(4):652-657.
- 392 32. Schettino GP, Tucci MR, Sousa R, Valente Barbas CS, Passos Amato MB, Carvalho CR. Mask  
393 mechanics and leak dynamics during noninvasive pressure support ventilation: a bench study.  
394 *Intensive Care Med* 2001; 27(12):1887-1891.

- 395 33. Epstein JB, Chow K, Mathias R. Dental procedure aerosols and COVID-19. *Lancet Infect Dis* 2021;  
396 21(4):e73.
- 397 34. Mick P, Murphy R. Aerosol-generating otolaryngology procedures and the need for enhanced PPE  
398 during the COVID-19 pandemic: a literature review. *J Otolaryngol Head Neck Surg* 2020; 49(1):29.
- 399 35. Wilson NM, Norton A, Young FP, Collins DW. Airborne transmission of severe acute respiratory  
400 syndrome coronavirus-2 to healthcare workers: a narrative review. *Anaesthesia* 2020; 75(8):1086-  
401 1095.
- 402 36. Kisielinski K, Giboni P, Prescher A, Klosterhalfen B, Graessel D, Funken S, Kempfski O, Hirsch O. Is a  
403 Mask That Covers the Mouth and Nose Free from Undesirable Side Effects in Everyday Use and  
404 Free of Potential Hazards? *Int J Environ Res Public Health* 2021; 18(8).
- 405 37. Rothe H, Fautz R, Gerber E, Neumann L, Rettinger K, Schuh W, Gronewold C. Special aspects of  
406 cosmetic spray safety evaluations: principles on inhalation risk assessment. *Toxicol Lett* 2011;  
407 205(2):97-104.
- 408 38. Tha EL, Canavez A, Schuck DC, Gagosian VSC, Lorencini M, Leme DM. Beyond dermal exposure:  
409 The respiratory tract as a target organ in hazard assessments of cosmetic ingredients. *Regul*  
410 *Toxicol Pharmacol* 2021; 124:104976.
- 411 39. Final Report on the Safety Assessment of Candelilla Wax, Carnauba Wax, Japan Wax, and  
412 Beeswax. *J Am Coll Toxicol* 1984; 3(3).
- 413 40. Arnesdotter E, Rogiers V, Vanhaecke T, Vinken M. An overview of current practices for regulatory  
414 risk assessment with lessons learnt from cosmetics in the European Union. *Crit Rev Toxicol* 2021;  
415 51(5):395-417.
- 416 41. Choksi NY, Truax J, Layton A, Matheson J, Mattie D, Varney T, Tao J, Yozzo K, McDougal AJ, Merrill  
417 J, Lowther D, Barroso J, Linke B, Casey W, Allen D. United States regulatory requirements for skin  
418 and eye irritation testing. *Cutan Ocul Toxicol* 2019; 38(2):141-155.
- 419 42. Filaire E, Nachat-Kappes R, Laporte C, Harmand MF, Simon M, Poinot C. Alternative in vitro  
420 models used in the main safety tests of cosmetic products and new challenges. *Int J Cosmet Sci*  
421 2022; 44(6):604-613.
- 422 43. Hardwick RN, Betts CJ, Whritenour J, Sura R, Thamsen M, Kaufman EH, Fabre K. Drug-induced skin  
423 toxicity: gaps in preclinical testing cascade as opportunities for complex in vitro models and  
424 assays. *Lab Chip* 2020; 20(2):199-214.
- 425 44. Nabarretti BH, Rigon RB, Burga-Sanchez J, Leonardi GR. A review of alternative methods to the  
426 use of animals in safety evaluation of cosmetics. *Einstein (Sao Paulo)* 2022; 20:eRB5578.
- 427 45. Pistollato F, Madia F, Corvi R, Munn S, Grignard E, Paini A, Worth A, Bal-Price A, Prieto P, Casati S,  
428 Berggren E, Bopp SK, Zuang V. Current EU regulatory requirements for the assessment of  
429 chemicals and cosmetic products: challenges and opportunities for introducing new approach  
430 methodologies. *Arch Toxicol* 2021; 95(6):1867-1897.
- 431 46. Riebeling C, Luch A, Tralau T. Skin toxicology and 3Rs-Current challenges for public health  
432 protection. *Exp Dermatol* 2018; 27(5):526-536.

433

434

435

436

437

## 438 **Figure Legends**

### 439 **Figure 1. Physical characterization of anti-fogging coating**

440 (A.) CAD of the contact angle apparatus for 3D printing (B.) CAD of the sliding angle module for  
441 3D printing (C.) 3D printed models of contact and sliding angle testing apparatus (D.) Image of  
442 the contact angle assessment showing droplet generation and analysis. Inset shows the digital  
443 analysis of contact angle  $\phi$  using NIH ImageJ (E.) Digital image analysis showing the sliding angle  
444 measurement using NIH ImageJ (F.) transmittance set-up using a diode laser and optical power  
445 meter with the sensor.

### 446 **Figure 2. Anti-fogging solution formulation and characterization**

447 (A.) Tabular outline of the formulation depicting ratios of carnauba and beeswax in acetone and  
448 methanol used to coat PETG plastic sheets (B. and C.) Contact angle assessment of Acetone and  
449 Methanol formulations at various concentrations (D and E) Sliding angle analysis of Acetone and  
450 Methanol formulations at various concentrations (F and G) Transmission of diode laser for  
451 transmittance assessment of Acetone and Methanol formulations at various concentrations. (I.)  
452 Digital image of an uncoated, Acetone and Methanol formulations applied to the PETG sheet.  
453 Data are shown as Mean and SD and representative of at least two independent studies. Statistical  
454 significance was determined using two-way analysis of variance (ANOVA) among different  
455 treatments using Bonferroni's multiple comparison test ( $n = 3$ ). Statistical significance is denoted  
456 as \*  $p < 0.05$ , \*\*  $p < 0.005$ , and \*\*\*  $p < 0.0005$ .

### 457 **Figure 3. Effects of Disinfection on anti-fogging coating integrity**

458 (A.) Contact angle assessment after various disinfection procedures (B.) Sliding angle analysis  
459 after various disinfection procedures (C.) transmittance after various disinfection procedures. Data  
460 are shown as Mean and SD and representative of at least two independent studies. Statistical  
461 significance was determined using two-way analysis of variance (ANOVA) among different  
462 treatments using Bonferroni's multiple comparison test ( $n = 3$ ). Statistical significance is denoted  
463 as \*  $p < 0.05$ , \*\*  $p < 0.005$ , \*\*\*  $p < 0.0005$ , and \*\*\*\*  $p < 0.00005$ .

464

465

466 **Figure 4. Durability testing of anti-fogging coating following contact testing**

467 (A.) CAD of contact testing apparatus used for wear testing analysis (B.) 3D printed model of the  
468 assembled contact testing apparatus (C.) Outline of the eminent forces determining the contact  
469 force on PETG surfaces. The contact angle (D.), sliding angle (E.), and transmittance (F.) analysis  
470 before and after contact testing (G.) Scanning electron microscopy images of the uncoated and  
471 coated surfaces before and after contact testing. Data are shown as Mean and SD and representative  
472 of at least two independent studies. Statistical significance was determined using the Students' T-  
473 test (n = 3). Statistical significance is denoted as \*  $p < 0.05$ .

474

475 **Figure 5. Clear face shields and masks**

476 A clear mask design with filter unit in medium (A.) and large (B.) sizes. The 3D printed clear face  
477 shields are shown to accommodate different dental operating loupes such as Eclipse (C.), Vision,  
478 Surgitel and Orascoptic (D.). Images are provided with consent from lab volunteers from the  
479 website [www.buffalo3dppe.com](http://www.buffalo3dppe.com).

# Figure 1

Figure 3. Effects of Disinfection on anti-fogging coating integrity

**(A.)** Contact angle assessment after various disinfection procedures **(B.)** Sliding angle analysis after various disinfection procedures **(C.)** transmittance after various disinfection procedures. Data are shown as Mean and SD and representative of at least two independent studies. Statistical significance was determined using two-way analysis of variance (ANOVA) among different treatments using Bonferroni's multiple comparison test ( $n = 3$ ). Statistical significance is denoted as \*  $p < 0.05$ , \*\*  $p < 0.005$ , \*\*\*  $p < 0.0005$ , and \*\*\*\*  $p < 0.00005$ .

Fig. 3

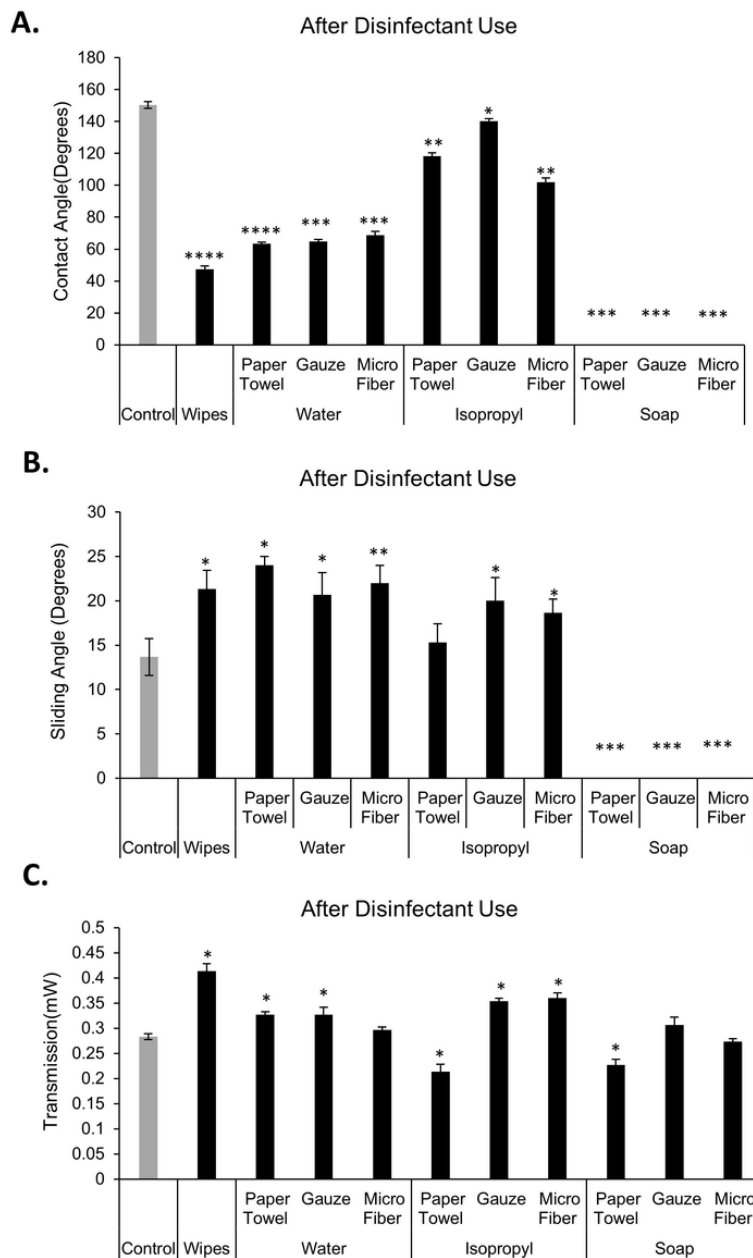


## Figure 2

Figure 5. Clear face shields and masks

A clear mask design with filter unit in medium (**A.**) and large (**B.**) sizes. The 3D printed clear face shields are shown to accommodate different dental operating loupes such as Eclipse (**C.**), Vision, Surgitel and Orascoptic (**D.**). Images are provided with consent from lab volunteers from the website [www.buffalo3dppe.com](http://www.buffalo3dppe.com) .

Fig. 5

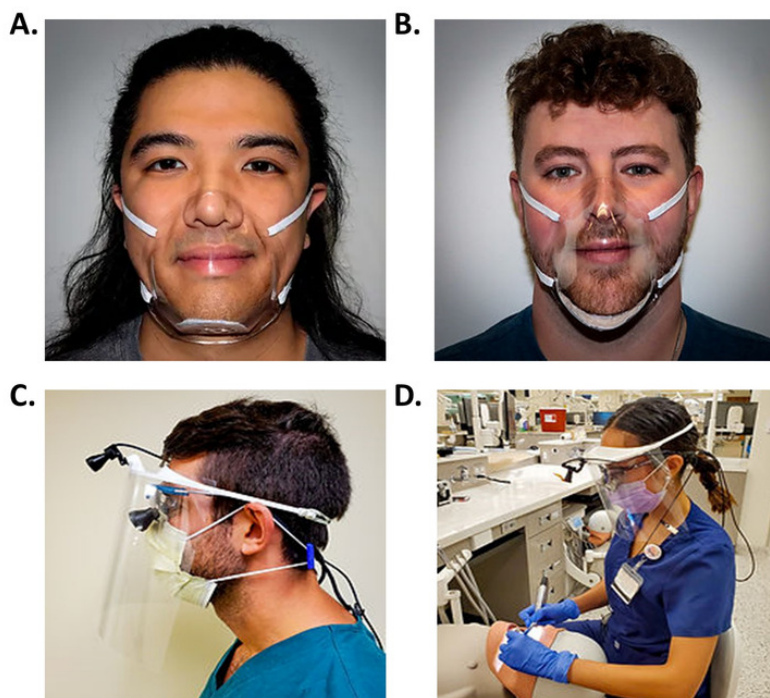


## Figure 3

Figure 4. Durability testing of anti-fogging coating following contact testing

(**A.**) CAD of contact testing apparatus used for wear testing analysis (**B.**) 3D printed model of the assembled contact testing apparatus (**C.**) Outline of the eminent forces determining the contact force on PETG surfaces. The contact angle (**D.**), sliding angle (**E.**), and transmittance (**F.**) analysis before and after contact testing (**G.**) Scanning electron microscopy images of the uncoated and coated surfaces before and after contact testing. Data are shown as Mean and SD and representative of at least two independent studies. Statistical significance was determined using the Students' T-test ( $n = 3$ ). Statistical significance is denoted as \*  $p < 0.05$ .

Fig. 4

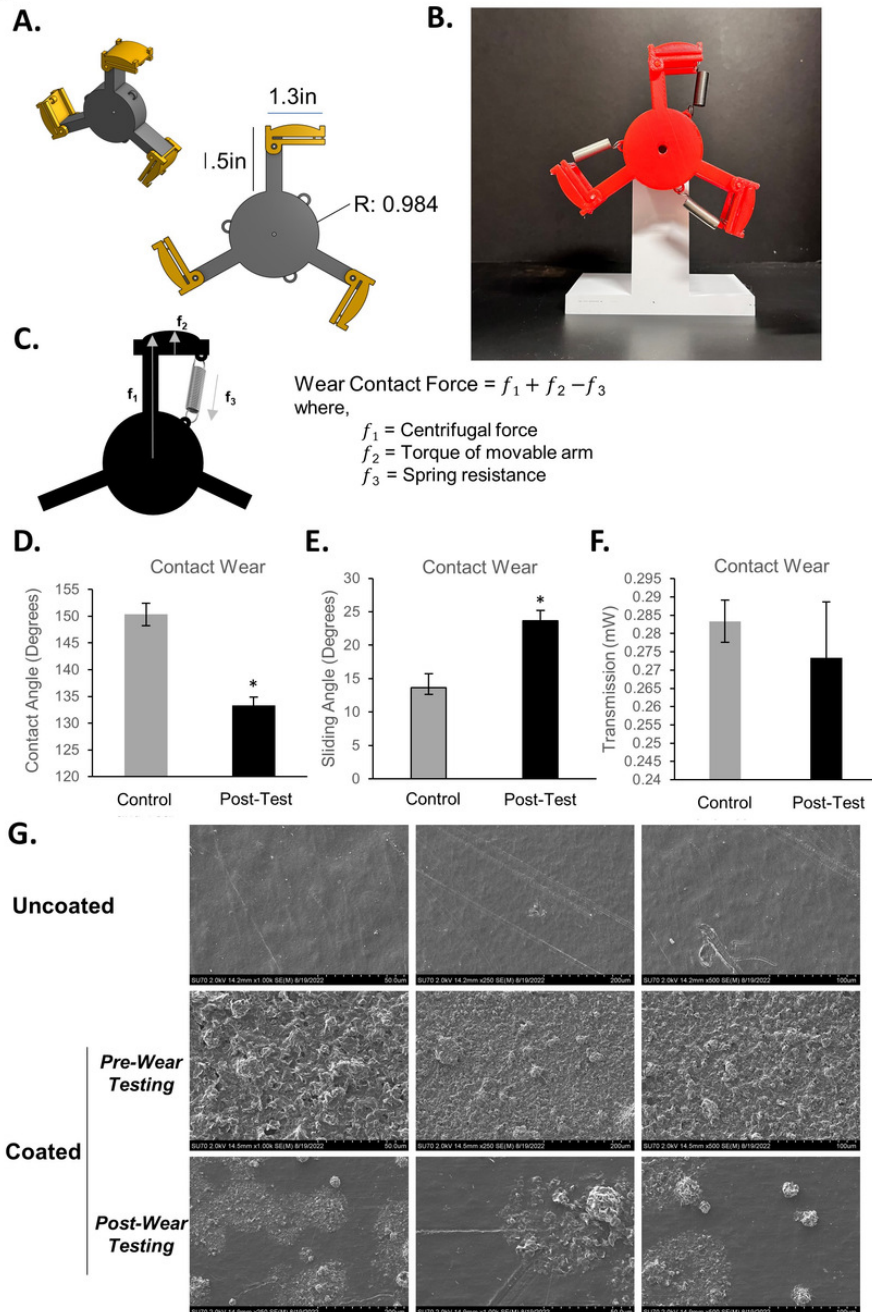


## Figure 4

Figure 2. Anti-fogging solution formulation and characterization

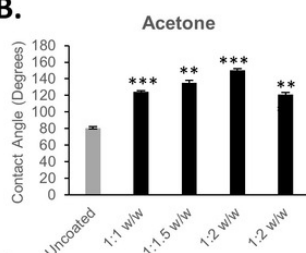
**(A.)** Tabular outline of the formulation depicting ratios of carnauba and beeswax in acetone and methanol used to coat PETG plastic sheets (**B.** and **C.**) Contact angle assessment of Acetone and Methanol formulations at various concentrations (**D** and **E**) Sliding angle analysis of Acetone and Methanol formulations at various concentrations (**F** and **G**) Transmission of diode laser for transmittance assessment of Acetone and Methanol formulations at various concentrations. (**I.**) Digital image of an uncoated, Acetone and Methanol formulations applied to the PETG sheet. Data are shown as Mean and SD and representative of at least two independent studies. Statistical significance was determined using two-way analysis of variance (ANOVA) among different treatments using Bonferroni's multiple comparison test ( $n = 3$ ). Statistical significance is denoted as \*  $p < 0.05$ , \*\*  $p < 0.005$ , and \*\*\*  $p < 0.0005$ .

Fig. 2

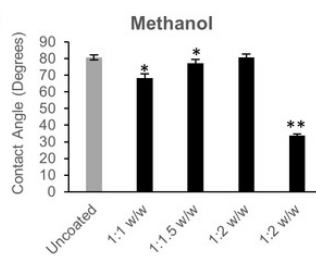
A.

Ratio	Carnauba (g)	Beeswax (g)	Acetone/Methanol (ml)
1:1	0.4375	0.4375	25
1:1.5	0.35	0.525	25
1:2	0.33	0.67	25
1:2 (HC)	0.417	0.833	25

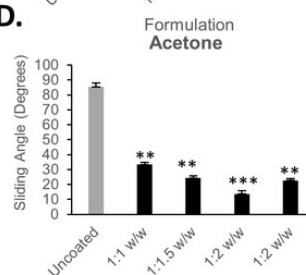
B.



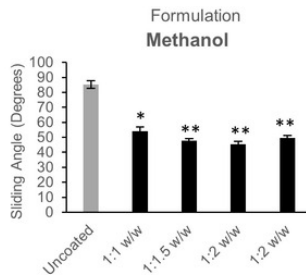
C.



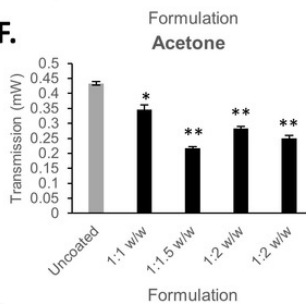
D.



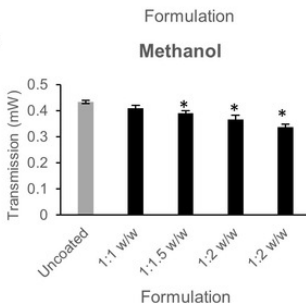
E.



F.



G.



I.



## Figure 5

Figure 1. Physical characterization of anti-fogging coating

(**A.**) CAD of the contact angle apparatus for 3D printing (**B.**) CAD of the sliding angle module for 3D printing (**C.**) 3D printed models of contact and sliding angle testing apparatus (**D.**) Image of the contact angle assessment showing droplet generation and analysis. Inset shows the digital analysis of contact angle  $\phi$  using NIH ImageJ (**E.**) Digital image analysis showing the sliding angle measurement using NIH ImageJ (**F.**) transmittance set-up using a diode laser and optical power meter with the sensor.

Fig. 1

